Temperature Dependence of Dissociative Recombination and Molecular-Ion Formation in He, Ne, and Ar Plasmas*

Che Jen Chen
Jet Propulsion Laboratory, California Institute of Technology, Pasadena, California
(Received 1 April 1968)

Recombination-dominated decaying plasmas in He, Ne, and Ar gases are produced in a discharge tube energized with a capacitor bank capable of delivering 3×10^3 J at 20 kV. The electron temperature, atom temperature, and electron number density as a function of time are measured by using a triple probe, a thin-film thermometer, and the triple probe and microwave apparatus, respectively. The atomic- and molecular-ion number densities are monitored by using a mass spectrometer. The electron-temperature dependence of the dissociative recombination coefficient α_2, and the atom-temperature dependence of the molecular-ion formation coefficient γ are calculated. The results indicate the following: (1) the electron-temperature dependence and absolute value of α_2 are both affected by the atom temperature of the plasma; a simplified physical model is proposed to explain this variation of dependence; the previous controversial experimental results published in the literature on this subject can be understood with the use of this physical model; and (2) the atom-temperature dependence of γ agrees with theoretical expectations.

I. INTRODUCTION

The existence of molecular ions of rare gases was first experimentally proved by Tuxen,[1] and later confirmed by several workers.[2-4] The most probable mechanisms for producing the molecular ions have been suggested to be a three-body process of atom-ion attachment[2,5]

$$R^+ + 2R \rightarrow R_2^+ + R, \tag{1}$$

and ionization attachment[3]

$$R^* + R \rightarrow R_2^+ + e, \tag{2}$$

where R and R^* are rare-gas atoms in ground state and excited states, respectively. Under present experimental conditions, according to the experimental results presented by Dahler *et al.*,[6] the mechanism responsible for the formation of R_2^+ is dominated by reaction of Eq. (1). In a rare-gas plasma, among others, the formation of the molecular ion and dissociative recombination, which is the reverse reaction of Eq. (2), takes place simultaneously. The formation and recombination reaction rates and their electron- and atom-temperature dependence (atom temperature assumed to be equal to that of ion) have been the subject of study for quite some time. Owing to the fact that there is lack of control over various parameters of the complicated processes in the plasma, the results published in the literature are rather controversial. For example, the electron temperature dependence of the dissociative recombination coefficient has been studied by several authors.[7-11] The results vary from $T^{-0.47}$ to $T^{-3/2}$ for a single gas (Ar) depending on the methods used to produce the plasma. Recently, Biondi *et al.*[12] have attempted to attribute the controversial results to differences in the atom temperature in the plasma of various experimenters. Experimental data on the atom-temperature dependence of the formation rate of the rare-gas molecular ions, to the author's knowledge, are still lacking in the published literature.

The present experiments are designed (1) to obtain information on the electron temperature dependence of the dissociative recombination rate of the rare-gas molecular ion with different atom temperatures, in order to study the possible dependence of the recombination process on the gas temperature, and (2) to measure atom-temperature dependence of the formation rate of the rare-gas molecular ion. The special features of this work are: (1) the electron temperature, electron density, relative atomic-ion and molecular-ion concentrations, and ion temperatures are measured simultaneously; (2) both dissociative recombination and molecular-ion production are taken into consideration in the decaying plasma; and (3) all the plasma parameters are measured locally.

II. THEORY OF THE EXPERIMENT

In a transient discharge tube energized with a capacitor bank, the principal processes prevailing in the tube are as follows. During the discharge period, the atomic ions and electrons are produced by electron-atom inelastic collision, and the molecular ions are produced by reaction as indicated in Eq. (1). In the afterglow decay period the dominant competing processes in the plasma are collisional-radiative recombination of electrons and atomic ions, dissociative recombination of electrons and molecular ions, and production of molecular ions (diffusion is negligible, as discussed in the next section). The rate equations are

$$dn_1/dt = p - \alpha_1 n_1 (n_1 + n_2) - \gamma n_a n_1 \tag{3}$$

and

$$dn_2/dt = \gamma n_a n_1 - \alpha_2 n_2 (n_1 + n_2), \tag{4}$$

where n_1 is atomic-ion number density, n_2 the molecular-ion number density, p the production rate of n_1 by electron impact, γ the molecular-ion

formation coefficient, α_1 the electron–atomic-ion recombination coefficient, n_a the neutral-atom density, and α_2 the molecular-ion dissociative recombination coefficient. Here, the equality $n_1+n_2=n_e$ (electron density) is assumed. After cessation of the discharge current, p can be neglected in Eq. (3). Then γ and α_2 can be solved in terms of α_1, n_1, n_2, dn_1/dt, and dn_2/dt as

$$\alpha_2 = -\left(\frac{dn_1}{dt}+\frac{dn_2}{dt}+\alpha_1 n_1(n_1+n_2)\right)\frac{1}{n_2(n_1+n_2)} \quad (5)$$

and

$$\gamma = -\left(\frac{dn_1}{dt}+\alpha_1 n_1(n_1+n_2)\right)\frac{1}{n_a n_1} . \quad (6)$$

All quantities in the right-hand side of Eqs. (5) and (6) are measured or calculated in the present setup except α_1, which is known only in some particular cases. However, under the present experimental conditions, the terms containing α_1 are negligible in comparison with the other terms as can be seen from the existing experimental[13] and calculated[14] values of α_1. Therefore, α_2 and γ can be obtained experimentally.

III. EXPERIMENT

The detailed description of the discharge tube and the techniques for measuring the electron density, electron temperature, and neutral gas temperature can be found elsewhere.[15] A brief summary of the technique, and a description of the additional instruments for the present study are given here.

The experimental setup is shown in Fig. 1. The discharge tube, which consists of a Pyrex bell jar about 45 cm in diameter and 50 cm in height, is energized with a capacitor bank capable of delivering energy up to 3000 J. The electrodes of the discharge tube are made of stainless steel. One of the electrodes serves as a table for the bell jar. The discharge current is triggered by a high-efficiency three-electrode trigger switch manufactured by Edgerton, Germeshausen, and Grier, Inc. The discharge pinch phenomena[16] cease to exist about 160 μsec after the cessation of the discharge current. The data in this experiment are taken after all disturbances have ceased. The apparatus is baked to a temperature of 250°C (the limitation of the O-ring seal) for about 48 h, and then is purged with the gases to be studied for about 48 h at flow rates of about 10 liter/h for He and Ar and 1 liter/h for Ne. Purging is stopped immediately before each run. The impurities of the three gases (He, Ne, and Ar) used in this study are 10 ppm, 12 ppm, and 10 ppm, respectively. The general features of the instrumentation are described as follows.

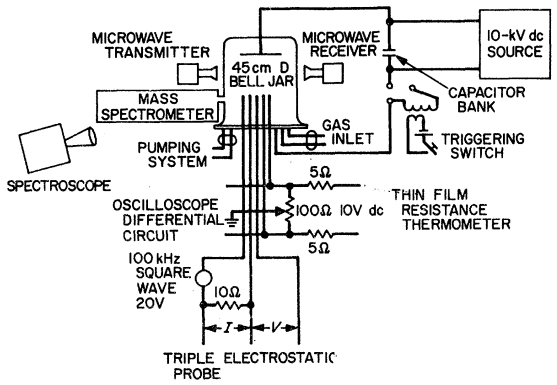

FIG. 1. Schematic diagram of experimental setup for electron-ion recombination study.

A. Electron Density, Electron- and Atom-Temperature Measurements

The dimension of the discharge tube is selected so that the diffusion effect is negligible. The electron temperature and electron density, as functions of time, are measured with a triple electrostatic probe.[17] Two sets of microwave equipment, 2.24×10^{10} Hz with cutoff electron density of 6.25×10^{12} cm^{-3}, and 8.97×10^{10} Hz with cutoff electron density of 1.0×10^{14} cm^{-3}, are used to calibrate the probe to remove the uncertainties of the dimension, accommodation coefficient, and other constants of the probe by observing the cutoff electron densities during the plasma decay. The electron temperature measured with the probe is counter checked with the spectral-line ratio method. The neutral-atom temperature is measured by using a thin-film copper-beryllium resistance thermometer.

B. Atomic-Ion and Molecular-Ion Number Density Measurement

A time-of-flight mass spectrometer (Bendix Corporation Basic Model 12) with a multichannel analog output system is used to monitor simultaneously the atomic-ion and molecular-ion concentrations. The sampling of the plasma into the mass spectrometer is arranged as shown in Fig. 2. The plasma leaks from the discharge tube into the mass spectrometer through a small hole about 0.1 cm in diameter. The differential pumping system is able to maintain a pressure ratio between the discharge tube and mass spectrometer about 10^5 or better. The ratio of the atomic-

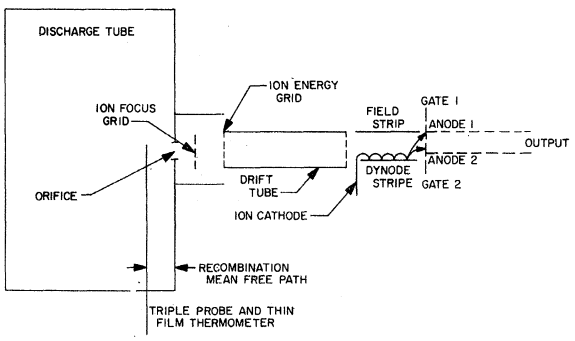

FIG. 2. Schematic diagram of mass spectrometer arrangement.

and molecular-ion concentrations is obtained from the ratio of the calibrated output signals I of the analog system for the specific mass numbers. The locations of the triple probe and the thin-film thermometer are adjusted to be about one recombination mean free path (see Appendix A) away from the wall, so that as far as the relative number densities of the different species in the plasma are concerned, the data obtained from the probe should register the same plasma properties as in the mass spectrometer. The mean free path of the plasma in the mass spectrometer is greater than the dimension of the instrument. No further reaction in the plasma occurs in the mass spectrometer, and the following relations prevail:

$$n_1/n_2 = I_1/I_2 = I_{12} = 1/I_{21}\,, \tag{7}$$

$$n_1 + n_2 = n_e\,, \tag{8}$$

$$n_1 = n_e/(1+I_{21}),\quad n_2 = n_e I_{21}/(1+I_{21})\,, \tag{9}$$

where I_{21} is obtained from the mass spectrometer measurement, and n_e from the triple probe measurement. Thus n_1 and n_2 give, respectively, the atomic- and molecular-ion number densities at the location where the triple probe and thermometer are situated. The atomic number density n_a is calculated by using the expression $n_a = P_i/kT_\gamma$, where P_i, the initial pressure of the discharge tube, is measured by using a thermocouple gauge; T_γ is the room temperature; and k is the Boltzmann constant.

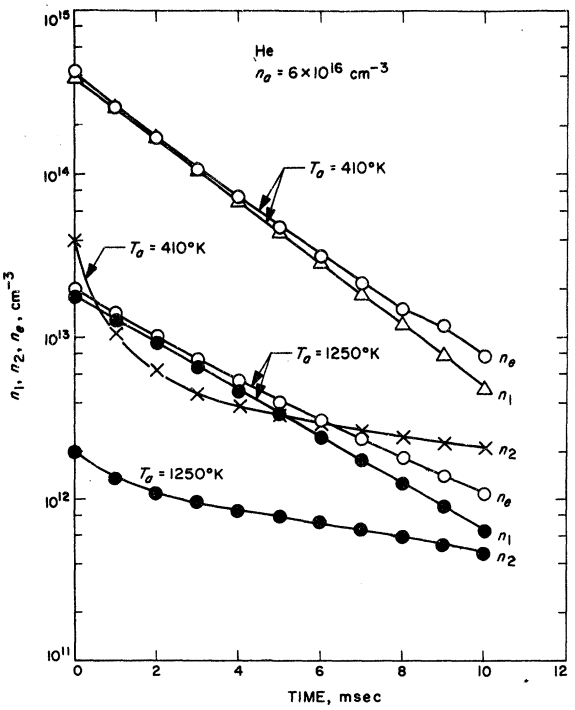

FIG. 3. Measured n_1, n_2, and n_e as a function of time for different T_a.

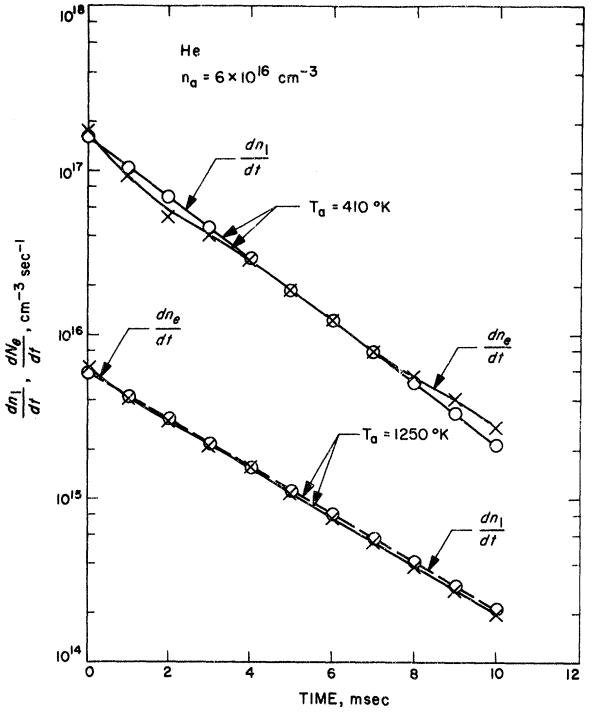

FIG. 4. dn_1/dt and dn_e/dt as a function of time for different T_a.

C. Evaluation of α_2 and γ and Their Electron-Temperature Dependence

The typical measured n_1, n_2, and n_e as functions of time t for He at two different values of T_a are shown in Fig. 3. The values of dn_e/dt and dn_1/dt, obtained in a computer by differentiating n_e and n_1 with respect to time, are shown in Fig. 4. The measured values of T_e as a function of time are shown in Fig. 5. The values of α_2 and γ/n_a calculated by using Eqs. (5) and (6), re-

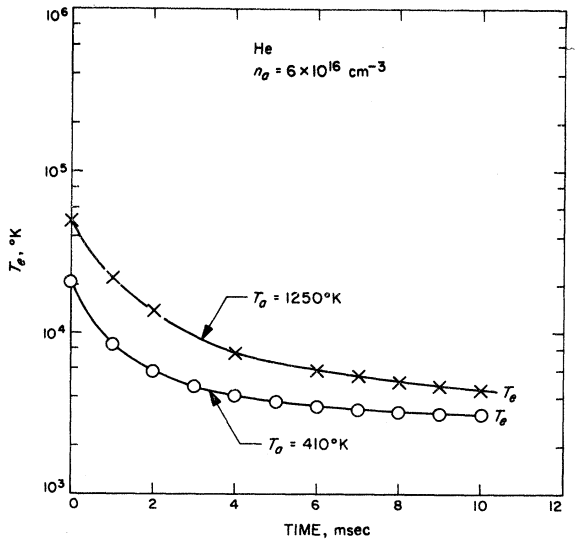

FIG. 5. Measured T_e as a function of time.

spectively, and the data depicted in Figs. 3 and 4 are shown in Figs. 6 and 7.

We note the following interesting features of these figures:

1. The atomic ions are the main constituent of the charged particles in the plasma, and both atomic-ion and electron densities follow approximately the same exponential decay law. These facts suggest that the dominant decay mechanisms of atomic ions (electron–atomic-ion recombination and diffusion are negligible) can be expressed by

$$R + R^+ + R \rightarrow R_2^+ + R,$$

and $$R_2^+ + e \rightarrow R + R.$$

It is plausible that in a plasma of high electron temperature and high electron density, such as is obtained in the present experiment, the electron-atom inelastic collisions are expected to be the dominating ionization process in the plasma. The metastable atoms are more likely to be further excited to higher bound or continuum states by electron-atom collision rather than by metastable atom-atom collisions as in the case of lower-energy and -density plasma discussed in Ref. 18.

2. The atom or ion temperature T_a in a single run is observed to be a constant in the measurement period. Change of T_a can only be accomplished by changing the discharge conditions (condenser voltage, discharge current, pressure of the gas, etc.). The constancy of T_a is expected to be the case. The atom temperature is raised mostly by the ohmic heating during the discharge period. The energy transfer from electrons to atoms or ions through electron-atom or electron-ion elastic collisions in the whole measurement period has been estimated to be only a very small fraction (~ $1/10^4$–$1/10^2$) of the gas energy content, which is calculated from the measured data of atom temperature and gas pressure. The convection and conduction heat losses are negligible in the present experimental setup during the observation time interval of the order of a few milliseconds. It is worthwhile to mention here that the resistance thermometer is slightly heated by the current flowing in the strip (380°K), so the measurable gas temperature must be higher than the initial strip temperature 380°K.

3. For a constant gas pressure, the initial electron density increases, and the electron temperature decreases with increasing discharge current in the range of the present experiment. The peak current density of the discharge current pulse in the present experiment is about 60–320 A/cm², so the discharge characteristic is in the negative-resistance regime.[19] The oscillograms shown in Fig. 8 depict clearly the negative-resistance characteristic during the early discharge period, where the discharge current increases as the voltage decreases. In the initial few microseconds, the voltage across the discharge tube drops from a few thousand volts to a few hundred volts. The rate of decrease of the discharge voltage is faster when the discharge current is larger. Following the current peak, the voltage drops below the voltage able to maintain the arc and the discharge process ceases. The voltage and current characteristics are then those of a circuit maintained by a decaying capacitor, where a small current is flowing in the afterglow plasma. Under the present experimental conditions, an increase of the peak discharge current is accompanied with the decrease of the discharge-maintaining voltage. It is understood[19] that the initial electron density increases as the discharge current increases, and the initial electron temperature decreases as the

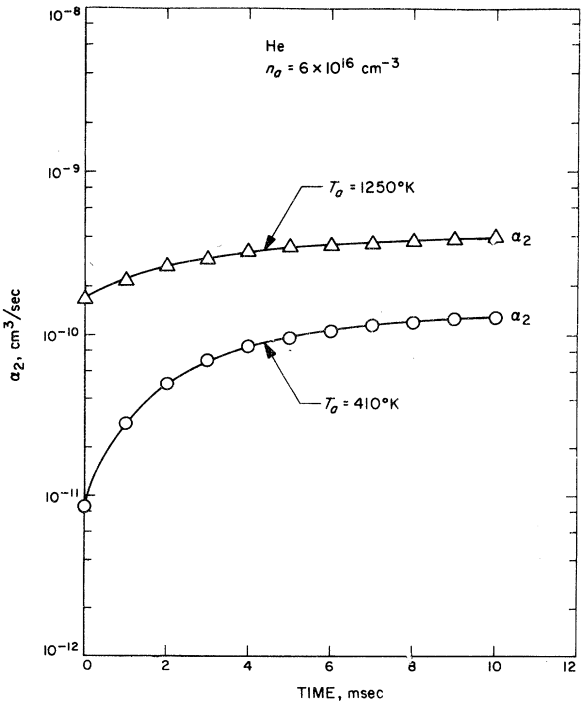

FIG. 6. α_2 as a function of time.

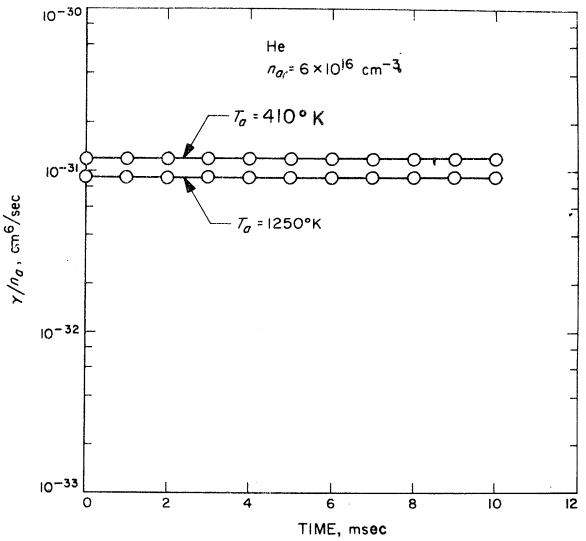

FIG. 7. γ/n_a as a function of time.

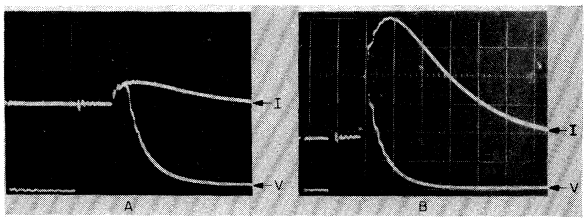

FIG. 8. Two oscillograms showing typical discharge conditions for He (see also Table I). Ordinate: discharge current I in 1170 A/main division, discharge voltage V in 220 V/main division; abscissa: time in 10 μsec/main division.

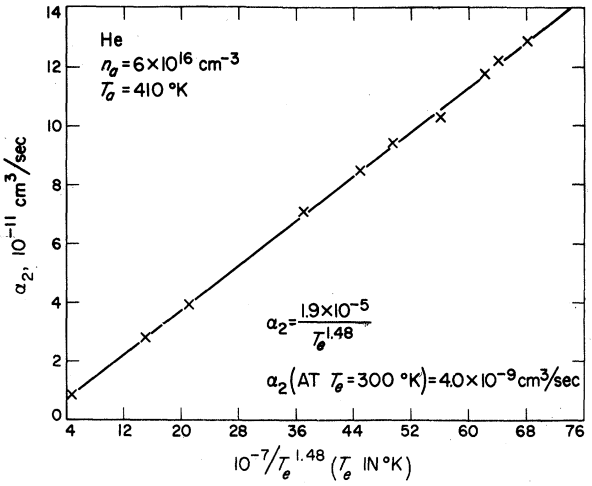

FIG. 9. α_2 as a function of T_e for He at $T_a = 410$°K.

electric field (proportional to the maintaining voltage minus anode and cathode drops) in the positive column decreases. Therefore, the initial electron density increases, and the initial electron temperature decreases, as the discharge current increases. The parameters for the two oscillograms of Fig. 8 are shown in Table I. However, in a small discharge current regime, both the electron density and the electron temperature can increase as the discharge current increases.

4. The values of α_2 increase as electron temperature decreases. Furthermore, in the plot of the values of α_2 against T_e^{-n}, a linear trend can always be obtained by adjusting the value of n. This suggests that the data of α_2 can be fitted into the form $\alpha_2 = K/T_e^n$. (The theoretical calculation also indicates the same possibility as shown in Sec. IV.) For example, in doing so, for the data presented in Figs. 3–6, straight lines as shown in Figs. 9 and 10 are obtained. The values of n and K thus obtained are as follows: $n = 1.48$, $K = 1.9\times10^{-5}$ cgs units, for $T_a = 410$°K; and $n = 0.36$, $K = 8.7\times10^{-9}$ cgs units for $T_a = 1250$°K. It is interesting to note that n, K, and α_2 (at $T_e = 300$°K) vary as T_a changes. The dependence of n, K, and α_2 on T_a will be discussed in Sec. IV.

5. The values of γ as expected are independent of T_e within the experimental error as shown in Fig. 7, and increase as T_a decreases. Both experimental data and theoretical calculation (Appendix B) indicate that γ can be fitted with the form $\gamma = K'/T_a^n$. The straight line obtained by plotting γ against $1/T_a^n$ for He gas with $n = 0.24$ is shown in Fig. 11. The result of reduction of the complete data for three rare gases by using the same procedures as described above is presented in Sec. IV.

IV. RESULTS AND DISCUSSION

A. Coefficient of Dissociative Recombination

As described in the last section, the data obtained from the present setup for values of α_2 can be expressed empirically as

$$\alpha_2 = K(T_a)/T_e^{n(T_a)}. \tag{10}$$

The values of K and n as a function of T_a for the three rare gases He, Ne, and Ar are shown in Fig. 12 and Fig. 13 (Refs. 20–23). The extrapolated values of the dissociative recombination coefficient at 300°K also manifest their dependence on T_a as shown in Fig. 14 (Refs. 24–30). The results can be explained qualitatively as follows.

The dissociative recombination coefficient α_2 can be expressed as[31]

$$\alpha_2 = CT_e^{-3/2}\frac{g_0(T_e)}{\tau_a + g_0(T_e)\tau_p}. \tag{11}$$

in which C stands for $h^3/2(2\pi mk)^{3/2}\,W/W^+$ (where h is the Planck constant, m the electronic mass, k the Boltzmann constant, W and W^+ the statistical weights of the relevant electronic states of the neutral molecule and of the molecular ion, respectively), τ_a for the lifetime against autoionization of the captured electron, τ_p for the lifetime of the mutual-repulsion stabilization process in which the constituent atoms move

TABLE I. Parameters for the two oscillograms of Fig. 8.

Picture in Fig. 8	Condenser bank initial voltage (V)	Max (I/A)[a] (A/cm^2)	V at max I (V)	Initial T_e (°K)	Initial N_e (cm^{-3})	T_a (°K)
A	4800	59.0	450	4.8×10^4	2×10^{13}	1250
B	19000	310	210	2×10^4	4×10^{14}	410

[a] A = electrode area = 290 cm^2.

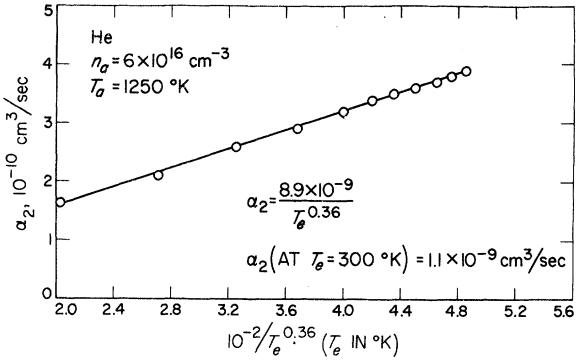

FIG. 10. α_2 as a function of T_e for He at $T_a = 1250$ °K.

apart by virtue of the Franck-Condon principle, and

$$g_0(T_e) = \int_0^\infty f_0(\epsilon) e^{-\epsilon/kT} d\epsilon \,, \tag{12}$$

with $|\Psi_0(R)|^2 \, dR/d\epsilon = f_0(\epsilon)$. (13)

In the last expression $\Psi_0(R)$ is the normalized vibrational wave function of the molecular ion, R the internuclear distance, and ϵ the energy supplied by the electron in vertical transition from a molecular ionic state to a repulsive state as shown in Fig. 15. It can be seen from the potential energy curves of states that

$$f_0(\epsilon) \to 0 \quad \text{as} \quad \epsilon \to \infty \,,$$

$$\text{and} \quad f_0(\epsilon) \to m \quad \text{as} \quad \epsilon \to 0 \,, \tag{14}$$

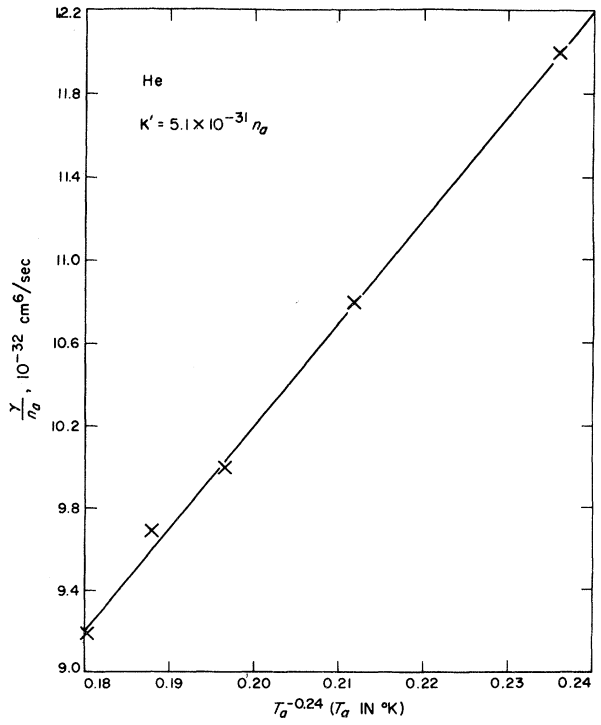

FIG. 11. γ/n_a as a function of T_a.

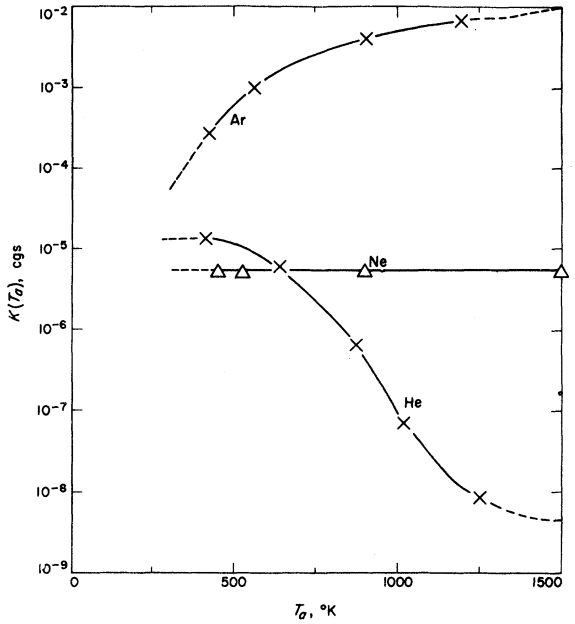

FIG. 12. $K(T_a)$ as a function of atom temperature T_a.

where m is a finite number or zero and its value depends upon the relative configuration between the two potential curves and the values of the vibrational wave functions.

After integrating by parts and imposing the conditions indicated in Eq. (14), Eq. (12) becomes

$$g_0(T_e) = a(kT_e) + b(kT_e)^2 + c(kT_e)^3 + \cdots \,, \tag{15}$$

where a, b, c, ... are equal to $f_0(0)$, $f_0'(0)$, $f_0''(0)$, ..., respectively. Here $f_0(\epsilon)$ is assumed to be a well-behaved function. Thus

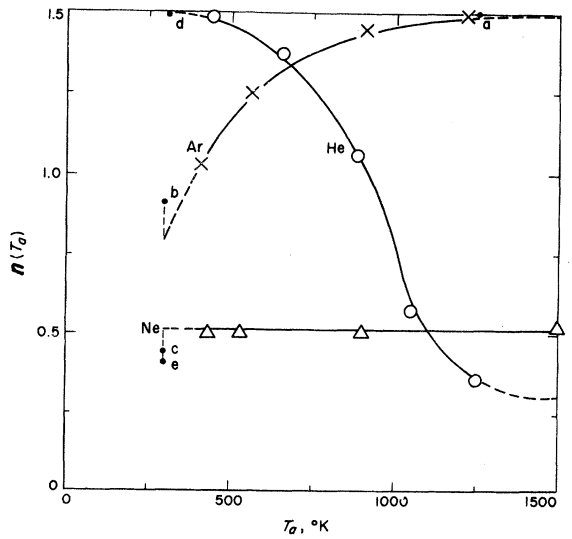

FIG. 13. $n(T_a)$ as a function of atom temperature T_a. Point a (Ref. 21), point b (Ref. 22), point c (Ref. 22), point d (Ref. 20), point e (Ref. 23).

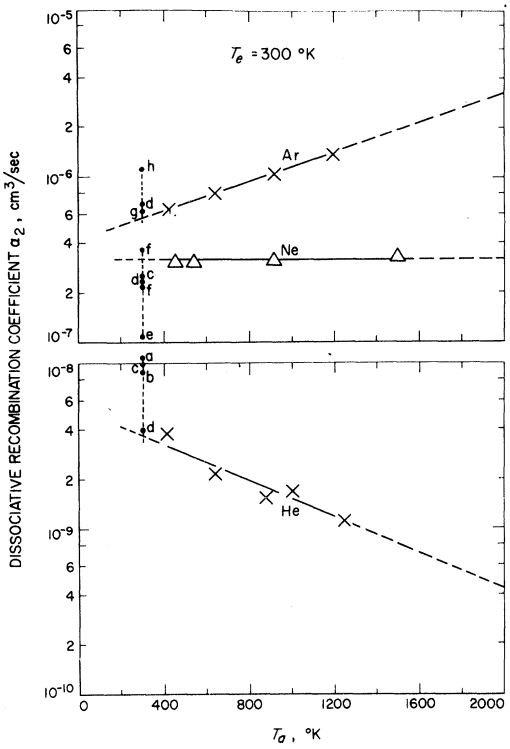

FIG. 14. α_2 as a function of atom temperature T_a. Point a (Ref. 24), point b (Ref. 25), point c (Ref. 26), point d (Ref. 27), point e (Ref. 28), point f (Ref. 28), point g (Ref. 29), point h (Ref. 30).

$$\alpha_2 = \frac{C}{T_e^{-3/2}} \frac{a(kT_e)+b(kT_e)^2+\cdots}{\tau_a+[a(kT_e)+b(kT_e)^2+\cdots]\tau_p}. \quad (16)$$

Since τ_a in most cases is of the order of 10^{-13} sec and τ_p of the order of 10^{-14} sec,[31] the values of $[a(kT_e)+b(kT_e)^2+\cdots]$ play an important role in the electron-temperature dependence of α_2. If $\tau_a \ll (\tau_p \text{ term})$, $n=\frac{3}{2}$. On the other hand, if $(\tau_p \text{ term}) \ll \tau_a$, and only the first-order term in $g_0(T_e)$ is considered, then $n=\frac{1}{2}$; however, when the higher-order terms in $g_0(T_e)$ become influential, n can be less than $\frac{1}{2}$.

To estimate the value of $f_0(0)$, the following harmonic oscillator vibrational wave function[32,33] is used

$$|\Psi_0(R)|^2=(2^v v!)^{-\frac{1}{2}}(\alpha/\pi)^{\frac{1}{4}}e^{-\alpha(R-R_0)^2}, \quad (17)$$

where $\alpha=4\pi^2\mu cw/h$ (μ is the reduced mass of the atom, c the velocity of light, w the vibration constant, h the Planck constant), and R_0 is the equilibrium internuclear distance. According to Refs. 31 and 32, w is approximately equal to 1000 cm^{-1}. The maximum values of $|\Psi_0(R)|^2$ for the gases studied are of the order of 10^9 cm^{-3}, and $dR/d\epsilon$ is estimated to be of the order of 10^6 cm/erg. Thus under certain conditions, the term containing τ_p in the denominator of Eq. (16) can be greater than τ_a. For example, if

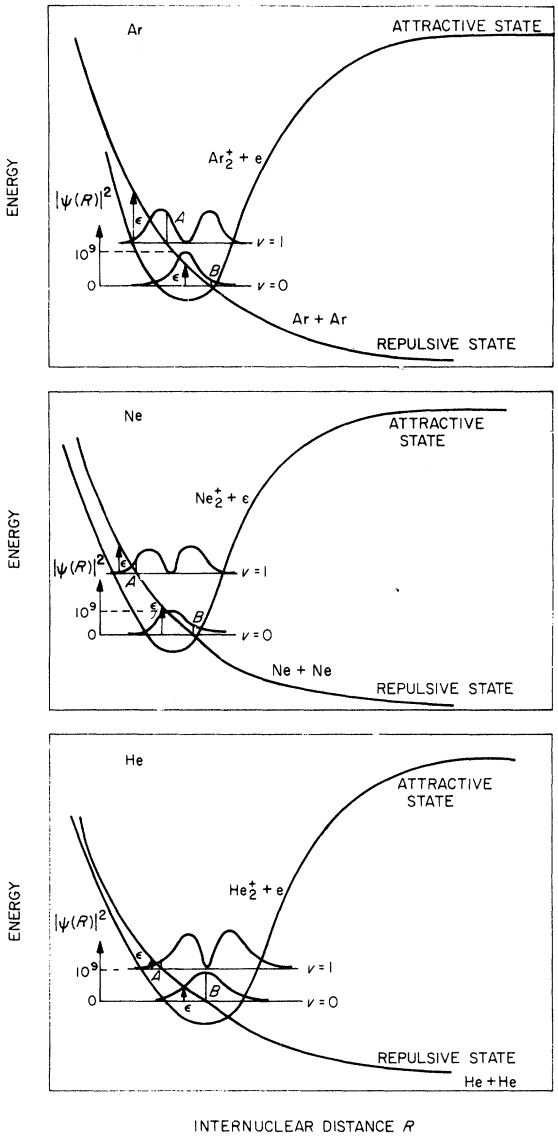

FIG. 15. Schematic diagram of the potential curves for He_2^+, Ne_2^+, and Ar_2^+.

$$\tau_a=10^{-13}\text{ sec},\quad \tau_p=10^{-14}\text{ sec (Ref. 14)},$$
$$|\Psi_0(R)|^2=10^9,\quad \frac{dR}{d\epsilon}=10^5\text{ cm/erg},\quad T_e=5000°\text{K},$$

then the term containing τ_p is greater than τ_a. In this case, the T_e dependence of α_2 appears to be as if the mutual-repulsion stabilization process is the limiting step in the dissociative recombination reaction and $n=\frac{3}{2}$. Of course, τ_a can be greater than τ_p term under a different condition. In this case, $n=\frac{1}{2}$ or $<\frac{1}{2}$, depending on the higher-order terms in $g_0(T_e)$.

To explain the T_a dependence of n and K, reference is made to Fig. 14 for the following three cases:

(1) He: At room temperature, it is reasonable to assume that the vibrational states are in the ground state $v=0$. The repulsive-potential curve

is assumed to intersect the $v=0$ state at the middle point as shown in Fig. 15 (He, B) where $\psi_2(R)^2$ is a maximum at $\epsilon=0$. The τ_p term in Eq. (16) may become larger than τ_a. As can be seen from Eq. (16), the electron temperature dependence of the dissociative recombination coefficient in this case obeys the $n=\frac{3}{2}$ relation. For this lower T_a case, the general trend both in absolute value and electron temperature dependence of α_2 agrees fairly well with the work of Chen *et al.*[20] whose results for He at 300°K are $\alpha_2=8\times10^{-9}$ cm³/sec, $n=\frac{3}{2}$. As the gas temperature is raised, the higher vibrational levels are populated. For instance, if at a moderate gas temperature T_a somewhere near 1000°K the transition to the repulsion states originates predominantly from the first-excited vibration state $v=1$, and if the intersection of the repulsive-potential curve with the level of the first-excited state is at a point where $|\psi_0(R)|^2$ is small, as shown in Fig. 15 (He, A), then the τ_a can be greater than the τ_p term. The electron-temperature dependence of α_2, in this case, obeys the $n=\frac{1}{2}$ relation. Furthermore, when the second term in $g_0(T_e)$ is sufficiently large to influence the value of $g_0(T_e)$, the electron temperature dependence of $g_0(T_e)$ appears to be a higher order than linear. Therefore n can be less than $\frac{1}{2}$, which explains the results obtained in the present work where $n=0.36$ at $T_a=1250$°K. Since α_2 is directly proportional to $g_0(T_e)$, and $g_0(T_e)$ is influenced by the higher vibrational level populations which are determined by T_a, the T_a dependence of α_2 can readily be understood.

(2) Ne: If the repulsive-potential curve intersects the levels $v=0$ and $v=1$ at points where $|\psi_0(R)|^2$ has about the same small value, as shown in Fig. 15 (Ne, A and B), the values of n and K should be insensitive to T_a. The present experimental results support this hypothesis. At $T_a=300$°K, satisfactory agreement is shown between the present results and the work of Frommhold, Biondi, and Mehr,[34] where $\alpha_2=1.7\times10^{-7}$ cm³/sec at $T_e=300$°K, $n=0.43$.

(3) Ar: If in this case, the situation is just the opposite as that described in (1) above for He, and A is greater than B as shown in Fig. 15 (Ar, A and B), then, $n=\frac{3}{2}$ at higher T_a and $n\approx\frac{1}{2}$ at lower T_a. This trend is supported by both the present experimental results and the results of Fox and Hobson[21] ($\alpha_2=3\times10^{-7}$ cm³/sec at $T_e=300$°K, $n=\frac{3}{2}$ at $T_a=1-3\times10^3$°K) and Mehr and Biondi[22] ($\alpha_2=8.3\times10^{-7}$ cm³/sec at $T_e=300$°K, $n=0.7$ at $T_a=300$°K).

The above description is a simplified physical model to explain the results obtained in this experiment. In fact, there are many more complicated processes taking place in the plasma. Several vibrational levels v may be important for higher gas temperatures. As pointed out by Bates,[31] in that case $g_0(T_e)$ should be replaced by a more complicated expression. Furthermore, account should be taken of the possible dependence of τ_p on ϵ and vibrational energies.

B. Molecular-Ion Production Rate

The T_a dependent coefficient of molecular-ion formation obtained from the present data for T_a ranging from 300 to 1500°K can be expressed as follows (for He as shown in Fig. 10):

$$\begin{aligned}
&\text{He: } \gamma=5.1\times10^{-31}\times n_a T_a^{-0.24} \text{ cm}^3/\text{sec},\\
&\text{Ne: } \gamma=3.1\times10^{-31}\times n_a T_a^{-0.23} \text{ cm}^3/\text{sec},\\
&\text{Ar: } \gamma=4.4\times10^{-32}\times n_a T_a^{-0.27} \text{ cm}^3/\text{sec}.
\end{aligned} \tag{18}$$

The values of γ/n_a for He, Ne and Ar at 300°K (γ normalized to a single atom) are

$$\begin{aligned}
&\text{He: } 1.3\times10^{-31} \text{ cm}^6/\text{sec},\\
&\text{Ne: } 8.5\times10^{-32} \text{ cm}^6/\text{sec},\\
&\text{Ar: } 9.4\times10^{-33} \text{ cm}^6/\text{sec}.
\end{aligned} \tag{19}$$

The first two values are in fairly good agreement with the results of Beaty and Patterson,[35] which are 1.1×10^{-31} and 5.8×10^{-31} cm⁶/sec, respectively. Their latest figure for Ne is 7×10^{-31} cm⁶/sec. The T_a dependence of γ agrees fairly well with the theoretical expectation (Appendix B). No electron-temperature dependence of γ can be established for the data obtained in this experiment.

ACKNOWLEDGMENT

The author is grateful to Gary Russell of the Jet Propulsion Laboratory for his advice and encouragement.

APPENDIX A

The collision frequency ν_R resulting in the dissociative recombination between molecular ions and electrons can be expressed as

$$\nu_R=C_e q_R n_e=\alpha_2 n_e, \tag{A1}$$

and that between molecular ions and neutral atoms ν_{ia} as

$$\nu_{ia}=C_i q_{ia} n_a, \tag{A2}$$

where C_e and C_i are the thermal speeds of the electrons and ions respectively, and q_R and q_{ia} are the cross sections for dissociative recombination and ion-atom elastic collisions, respectively (elastic collisions between ions and electrons are negligible because the degree of ionization is small).

The number of the ion-atom elastic collisions taking place between two dissociative recombination events is

$$N=\frac{\nu_{ia}}{\nu_R}. \tag{A3}$$

According to the three-dimensional random-walk theory,[36] the effective dissociative-recombination mean free path λ_R can be written as

$$\lambda_R=(8/3\pi)N^{1/2}\lambda_{ia}$$

$$= \frac{1.26\times10^{-4}(T_i/m_i)^{1/4}}{(\alpha_2 n_e q_{ia} n_a)^{1/2}}, \quad N \gg 1, \tag{A4}$$

where $\lambda_{ia} = 1/(q_{ia} n_a)$ is the mean free path for ion-atom collisions. The values of q_{ia} are taken from Varney's work.[37]

APPENDIX B

Under the premise that two different particles, A and B, will attach to each other if their total relative energy ever becomes negative (that is, if their kinetic energy of relative motion E ever becomes less than the potential energy of the system), Natanson[38] has refined Thomson's[39] calculation to obtain the rate of the event η to be

$$d\eta/dt \simeq \tfrac{17}{5}\pi n_A n_B r_1^3 \bar{v} = \gamma n_A n_B, \quad \lambda \gg e^2/kT_a, \quad \lambda \gg r_1, \tag{B1}$$

where $\bar{v}$ is the relative velocity of the particles, n_A and n_B the number densities of particles A and B, respectively, λ the mean free path of the particles, e the electronic charge, and r_1 the critical distance obeying the following relation

$$\tfrac{3}{2}kT_a = \int_{r_1}^{\infty} F\,dr, \tag{B2}$$

where F is the law of force between particles A and B.[40]

In carrying over this calculation to the molecular-ion formation case, F has the form[18]

$$F = \frac{\alpha e^2}{r^5}, \tag{B3}$$

where α is the polarizability of the atom. On integration, Eq. (B2) yields

$$r_1^4 = \frac{2\alpha e^2}{3kT_a}. \tag{B4}$$

From Eqs. (B1) and (B4), and since $\bar{v} \propto T_a^{1/2}$, γ can be expressed as

$$\gamma = |2\alpha e^2/3kT_a|^{3/4} \tfrac{17}{5}\pi\bar{v} \propto T^{-0.25}. \tag{B5}$$

In the last expression, the populations of the higher electronic states of the atoms are assumed to be small in comparison with that of the ground states, so that α is a constant independent of T_e and T_a. Otherwise α (which changes as the electronic states in the atom change) would be a function of T_a and T_e because of the dependence of the population of higher electronic states of the atoms on T_a and T_e.

---

*This work presents the results of one phase of research carried out in the Propulsion Research and Advanced Concepts Section of the Jet Propulsion Laboratory, California Institute of Technology, under Contract No. NAS 7-100, sponsored by the National Aeronautics and Space Administration.

[1]O. Tüxen, Z. Physik 103, 463 (1936).
[2]F. L. Arnot and M. B. M'Ewen, Proc. Roy. Soc. (London) A166, 543 (1938).
[3]J. A. Hornbeck and J. P. Molnar, Phys. Rev. 84, 621 (1951).
[4]A. V. Phelps and S. C. Brown, Phys. Rev. 86, 102 (1952).
[5]E. C. Beaty and P. L. Patterson, Phys. Rev. 137, 346 (1965).
[6]J. S. Dahler, J. L. Franklin, M. S. B. Munson, and F. H. Fields, J. Chem. Phys. 36, 3332 (1962).
[7]M. A. Biondi and S. C. Brown, Phys. Rev. 76, 1697 (1949).
[8]C. L. Chen, C. C. Leiby, and L. Goldstein, Phys. Rev. 121, 1391 (1961).
[9]K. B. Person and S. C. Brown, Phys. Rev. 100, 729 (1955).
[10]J. M. Anderson, Phys. Rev. 108, 898 (1958).
[11]L. Goldstein, J. M. Anderson, and G. L. Clark, Phys. Rev. 90, 486 (1952).
[12]M. A. Biondi *et al.*, private communication.
[13]S. C. Brown, Basic Data of Plasma Physics (Massachusetts Institute of Technology Press, Cambridge, Mass., 1961), p. 988.
[14]D. R. Bates, A. E. Kingston, and R. W. P. McWhirter, Proc. Roy. Soc. (London) A267, 297 (1962); and A270, 155 (1962).
[15]Che Jen Chen, Phys. Rev. 163, 1 (1967).
[16]R. G. Jahn and W. Von Jackowsky, Am. Inst. Aeron. Astron. J. 1, 1809 (1963).
[17]S. L. Chen and T. Sekignchi, J. Appl. Phys. 36, 2363 (1965).
[18]H. Myers, Phys. Rev. 130, 1639 (1963).
[19]Gordon Francis, in Handbuch der Physik, edited by S. Flügge (Springer-Verlag, Berlin, 1956), Vol. XXII, p. 114; J. D. Cobine, Plasma Conductors (Dover Publications, New York, 1958), pp. 93, 154, 234.
[20]C. L. Chen, C. C. Leiby, and L. Goldstein, Phys. Rev. 121, 1391 (1961).
[21]J. N. Fox and R. M. Hobosn, Phys. Rev. Letters 17, 161 (1966).
[22]F. J. Mehr and M. A. Biondi, in Proceedings of the Twentieth Annual Gaseous Electronics Conference, San Francisco, 1967 (unpublished), Paper No. B-3.
[23]W. Z. Hess, Naturforsch 20, 451 (1965).
[24]M. A. Biondi and S. C. Brown, Phys. Rev. 75, 1700 (1949).
[25]R. A. Johnson, B. T. McClure, and R. B. Holt, Phys. Rev. 80, 376 (1950).
[26]H. J. Oskam, Philips Res. Rept. 13, 401 (1958).
[27]H. J. Oskam and V. R. Mittelstadt, Phys. Rev. 132, 1445 (1963).
[28]R. B. Holt, J. M. Richardson, B. Howland, and B. T. McClure, Phys. Rev. 77, 239 (1950).
[29]M. A. Biondi, Phys. Rev. 129, 1181 (1963).
[30]A. Redfield and R. B. Holt, Phys. Rev. 82, 874 (1951).
[31]D. R. Bates, Atomic and Molecular Processes (Academic Press, Inc., New York, 1962), p. 262.
[32]G. Herzberg, Molecular Spectra and Molecular Structure (D. Van Nostrand Company, Inc., Princeton, New Jersey, 1950), Vol. I, 2nd ed., p. 77.

[33]J. G. Winans and E. C. G. Stuckelberg, Proc. Natl. Acad. Sci. U. S. 14, 867 (1928).
[34]L. Frommhold, M. A. Biondi, and F. J. Mehr, Phys. Rev. 165, 44 (1968).
[35]E. C. Beaty and P. Patterson, in Proceedings of the Sixth International Conference on Ionization Phenomena in Gases, Paris, 1963, edited by P. Hubert and E. Crémieu-Alcan (European Atomic Energy Community, 1964), Vol. I, p. 289.
[36]W. Feller, An Introduction to Probability Theory and Its Applications (John Wiley & Sons, Inc., New York, 1957), Vol. 1, 2nd ed., p. 327.
[37]R. N. Varney, Phys. Rev. 88, 362 (1952).
[38]A. L. Natanson, Zh. Techn. Fiz. 29, 1373 (1959) [English Transl.: Soviet Phys. – Tech. Phys. 4, 1263 (1959)].
[39]J. J. Thomson, Phil. Mag. 47, 337 (1924).
[40]E. W. McDaniel, Collision Phenomena in Ionized Gases (John Wiley & Sons, Inc., New York, 1964), p. 29.

PHYSICAL REVIEW VOLUME 177, NUMBER 1 5 JANUARY 1969

Collisional-Radiative Recombination of Ions and Electrons in High-Pressure Plasmas in Which the Electron Temperature Exceeds the Gas Temperature*

C. B. Collins
Southwest Center for Advanced Studies, Dallas, Texas
(Received 5 August 1968)

The recombination rate of electrons in a hypothetical helium-like plasma at high pressure is calculated for cases in which the gas temperature is fixed at 300°K, and the electron temperature is varied from 300 to 2000°K. Neutral collision-induced recombination and electron collision-induced recombination are considered for ranges of electron density from 10^8 to 10^{13} cm^{-3} and gas densities from 10^{16} to 10^{19} cm^{-3}. An inverse three-halves dependence of recombination coefficient on electron temperature is found for certain densities.

INTRODUCTION

Theoretical considerations of collisional-radiative recombination of ions and electrons have been recently extended[1,2] to include neutral collision-induced recombination of the type proposed by Bates and Khare,[3] as well as electron collision-induced recombination processes,[4] for the case of thermal equilibrium between the free electrons and the heavy particles. In many experimental situations, the temperature of the electrons is higher than that of the heavy particles, either as a result of external heating of the plasma by some means such as microwave pulses, or by heating as a consequence of internal-energy sources. Of particular interest in such cases is the dependence of the recombination rate coefficient on electron temperature.

This paper reports a further extension of recombination rate calculations to plasmas having a neutral temperature of 300°K, and an electron temperature varying from 300 to 2000°K. Idealized ions of mass 4, with hydrogenic energy levels, were used in the calculations. Since the electron collision-induced recombination mechanisms are only slightly sensitive to the nature of the ions undergoing recombination, recombination rates for these idealized ions should reasonably approximate the recombination of He^+ with electrons. Conversely, since the neutral collision part of the recombination process is mass dependent, only the qualitative aspects of the calculations would pertain to the recombination of other ions.

THEORY

The range of processes included in the calculations are essentially the same as those used by Deloche,[1,2]

$$X^+ + 2e \rightleftarrows X^*(p) + e, \tag{1}$$

$$X^+ + e + X \rightleftarrows X^*(p) + X, \tag{2}$$

$$X^+ + e \rightarrow X^*(p) + h\nu, \tag{3}$$

$$X^*(p) + e \rightleftarrows X^*(q) + e, \quad p > q, \tag{4}$$

$$X^*(p) + X \rightleftarrows X^*(q) + X, \quad p > q, \tag{5}$$

$$X^*(p) \rightarrow X^*(q) + h\nu, \quad p > q, \tag{6}$$

where $X^*(k)$ denotes the kth excited state of the neutral atom. Rate coefficients for processes (1) and (4) were calculated by the Gryzinski approximations,[5] rates for (3) were taken from Bates and Dalgarno,[6] and rates for (6) from Green *et al.*[7] Rates for (5) and the inverse of (2) were calculated

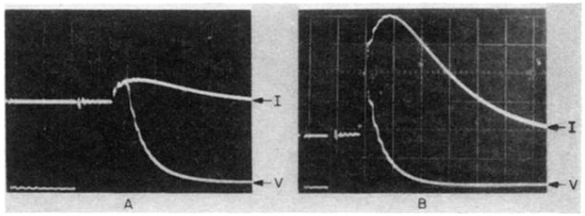

FIG. 8. Two oscillograms showing typical discharge conditions for He (see also Table I). Ordinate: discharge current I in 1170 A/main division, discharge voltage V in 220 V/main division; abscissa: time in 10 μsec/main division.